Heterodimerization of Insulin-like Growth Factor Receptor/Epidermal Growth Factor Receptor and Induction of Survivin Expression Counteract the Antitumor Action of Erlotinib

Floriana Morgillo, Jong Kyu Woo, Edward S. Kim, Waun Ki Hong, and Ho-Young Lee

Department of Thoracic/Head and Neck Medical Oncology, The University of Texas M.D. Anderson Cancer Center, Houston, Texas

Abstract

Epidermal growth factor receptor (EGFR) tyrosine kinase inhibitors (TKIs) have been used to treat non–small cell lung cancer (NSCLC). However, the overall response rate to EGFR TKIs is limited, and the mechanisms mediating resistance to the drugs are poorly understood. Here, we report that insulin-like growth factor-I receptor (IGF-IR) activation interferes with the antitumor activity of erlotinib, an EGFR TKI. Treatment with erlotinib increased the levels of EGFR/IGF-IR heterodimer localized on cell membrane, activated IGF-IR and its downstream signaling mediators, and stimulated mammalian target of rapamycin (mTOR)–mediated *de novo* protein synthesis of EGFR and survivin in NSCLC cells. Inhibition of IGF-IR activation, suppression of mTOR-mediated protein synthesis, or knockdown of survivin expression abolished resistance to erlotinib and induced apoptosis in NSCLC cells *in vitro* and *in vivo*. Our data suggest that enhanced synthesis of survivin protein mediated by the IGFR/EGFR heterodimer counteracts the antitumor action of erlotinib, indicating the needs of integration of IGF-IR–targeted agents to the treatment regimens with EGFR TKI for patients with lung cancer. (Cancer Res 2006; 66(20): 10100-11)

Introduction

The 5-year survival rate for lung cancer patients remains extremely poor (≤15; ref. 1), underscoring the need for more effective treatment strategies. Recently, new therapeutic approaches targeting signaling pathways involved in cell proliferation, apoptosis, angiogenesis, and metastasis have been investigated (2). Among the many potential target pathways, the epidermal growth factor (EGF) receptor (EGFR) signaling pathway has been studied most extensively because EGFR overexpression has been observed in a number of solid tumors, including 40% to 80% of non–small cell lung cancers (NSCLC; ref. 3). The EGFR signaling pathway activates the phosphatidylinositol 3-kinase (PI3K)/Akt and mitogen-activated protein kinase (MAPK) pathways, which play major roles in cell proliferation, survival, and transformation and in therapeutic resistance (4, 5). In addition, the EGFR pathway is implicated in angiogenesis, and cell invasion by its regulation of the expression and activity of matrix metalloproteinases (6, 7).

These findings indicate the therapeutic potential of inhibitors of EGFR tyrosine kinase activation. EGFR tyrosine kinase activity can be inhibited by antibodies against the extracellular domain of EGFR, such as cetuximab, or by small molecules that block the ATP binding site of the cytoplasmic domain, such as gefitinib (ZD1839, Iressa; AstraZeneca Pharmaceuticals, Macclesfield, United Kingdom) and erlotinib (Tarceva®; OSI Pharmaceuticals; Genentech, South San Francisco, CA). Both forms of EGFR inhibition have single-agent antitumor activity against previously treated NSCLC (3, 8–10). Erlotinib exhibits an antiproliferative effect at nanomolar concentrations and has induced apoptosis and reversible cell cycle arrest at G_1 (11). *In vivo* preclinical models have shown that erlotinib administration markedly reduces EGFR autophosphorylation and growth in human head and neck cancer xenografts (HN5 and A431 cells) in nude mice (11, 12). In addition, gefitinib, combined with standard chemotherapeutic agents and/or radiotherapy in preclinical studies, has inhibited EGFR activation, thus causing G_1 cell cycle arrest and contributing to synergistic growth inhibition (13).

Despite a similar chemical structure, these two EGFR tyrosine kinase inhibitors (TKIs) have provided contrasting results in phase III clinical trials, in which only erlotinib showed significantly improved survival compared with placebo (14–16). The response to gefitinib and erlotinib has been suggested to be associated with sex, smoking status, tumor histology, and somatic mutations of the EGFR ATP binding site (17, 18). Recent data have suggested that the insulin-like growth factor-1 receptor (IGF-IR) pathway is also implicated in the resistance of gefitinib and anti-EGFR monoclonal antibody (19, 20). However, to our knowledge, the mechanisms involved in the IGF-IR–mediated acquired resistance to erlotinib in NSCLC cells have not been completely defined. In this article, we report that erlotinib induce EGFR/IGF-IR heterodimerization on the cell membrane, transmitting a survival signal through IGF-IR and its downstream mediators PI3K/Akt and p44/42 MAPK to stimulate mammalian target of rapamycin (mTOR)–mediated synthesis of EGFR and antiapoptotic survivin proteins. Consequently, inactivation of IGF-IR, suppression of mTOR-mediated protein synthesis, or knockdown of survivin protein renders EGFR-overexpressing NSCLC cells sensitive to the erlotinib treatment.

Materials and Methods

Cells, reagents, and animals. The human NSCLC cell lines H596, H226B, H226Br, H460, H1299, A549, H358, H661, and H322 were from the American Type Culture Collection (Manassas, VA) and maintained in RPMI 1640 supplemented with 10% fetal bovine serum (FBS; Life Technologies, Gaithersburg, MD) in a humidified atmosphere with 5% CO_2. IGF and EGF were from R&D Systems (Minneapolis, MN). Erlotinib were prepared as 10 mmol/L stock solution in DMSO and stored at −20°C. LY294002

Note: Supplementary data for this article are available at Cancer Research Online (http://cancerres.aacrjournals.org/).

W.K. Hong is an American Cancer Society Clinical Research Professor. H-Y. Lee is a faculty member at the Graduate School of Biomedical Sciences.

Requests for reprints: Ho-Young Lee, Department of Thoracic/Head and Neck Medical Oncology, The University of Texas M.D. Anderson Cancer Center, Box 432, 1515 Holcombe Boulevard, Houston, TX 77030. Phone: 713-792-6363; Fax: 713-792-0430; E-mail: hlee@mdanderson.org.

doi:10.1158/0008-5472.CAN-06-1684

(an inhibitor of PI3K), PD98059 (an inhibitor of the MEK1), rapamycin, and AG1024, a TKI of IGF-IR, were from Calbiochem-Novabiochem (Alexandria, New South Wales, Australia); these inhibitors were prepared as 20 mmol/L stock solutions in DMSO and also stored at −20°C. Adenoviral vectors expressing survivin (Ad-survivin; ref. 21) or dnIGF-IR/482 [adenovirus-expressing, dominant-negative IGF-IR (Ad-dnIGF-IR)], a soluble extracellular domain of IGF-IR with an engineered stop codon at amino acid residue 482 (22), and control adenoviral vector [adenovirus-expressing empty vector (Ad-EV)] were amplified as described elsewhere (23). We confirmed increases in the levels of IGF-IR protein by Western blot assay with an antibody for the α-subunit (anti-IGF-IRα N-20, Santa Cruz Biotechnology, Santa Cruz, CA) using medium from the cells that were infected with Ad-dnIGF-IR because IGF-IR/482 has been shown to produce and release the truncated α-subunit of IGF-IR into the medium (22). The effect of the combination of erlotinib and Ad-dnIGF-IR on established s.c. tumor nodules was studied in athymic nude mice (Harlan Sprague-Dawley, Indianapolis, IN) in a defined pathogen-free environment. Six-week-old female mice were used in this study; mice with necrotic tumors or tumors ≥1.5 cm in diameter were euthanized.

Cell proliferation assay. Cells were treated with erlotinib, rapamycin, LY294002, PD98059, AG1024, Ad-dnIGF-IR, Ad-EV, or their combinations in the absence or presence of 10% FBS, EGF (50 ng/mL), or IGF (50 ng/mL). For the experiments with the viruses, cells were infected with 5 and 10 particle forming unit (pfu) for Ad-dnIGF-IR or Ad-EV, in serum-free medium for 2 hours and then incubated for 3 days in RPMI medium supplemented with 10% FBS in the absence or presence of the indicated concentrations of erlotinib. Cell proliferation was measured with the 3-(4,5-dimethylthiazol-2-yl)-2,5-diphenyltetrazolium bromide (MTT) assay. The drug concentrations required to inhibit cell growth by 50% were determined by interpolation from the dose-response curves. For defining the effect of the combined drug treatments, any potentiation was estimated by multiplying the percentage of cells remaining by each individual agent. The synergistic index was calculated as previously described (24). In the following equations, A and B are the effects of each individual agent, and AB is the effect of the combination. Subadditivity was defined as %AB / (%A × %B) < 0.9; additivity was defined as %AB / (%A × %B) = 0.9-1.0; and supra-additivity was defined as %AB / (%A × %B) > 1.0.

Clonogenic growth assay. The anchorage-dependent clonogenic growth assay was done by seeding NSCLC cell lines into six-well plates at low density (≈3×10^3 cells per well). Cells were either left uninfected or infected with 5 or 10 pfu/cell of Ad-dnIGF-IR or Ad-EV, incubated for 72 hours with different concentrations of erlotinib (0.1, 1.0, and 5.0 μmol/L), AG1024 (5 μmol/L), or combinations of the two drugs in serum-free RPMI medium in the absence or presence of IGF (50 ng/mL). Cells were replated in six-well plates and cultured in growth medium for 7 to 10 days, in a humidified atmosphere with 5% CO_2, at 37°C, and then colonies were fixed with 0.1% Coomassie blue (Bio-Rad Laboratories, Hercules, CA) in 30% methanol and 10% acetic acid. We then counted the number of colonies with >50 cells. For the anchorage-independent clonogenic growth assay, ~3×10^3 cells were suspended in 0.75 mL of 0.22% soft agar that was layered on top of 1 mL of 1% solidified agar in each well of 24-well plates. The plates were then incubated for 10 to 15 days in serum-free RPMI medium containing 0.1 or 1.0 μmol/L concentrations of erlotinib in the absence or presence of 10% FBS or IGF (50 ng/mL). The medium was changed daily during this period, at the end of which tumor cell colonies measuring at least 80 μm were counted under using a dissection microscope.

Cell cycle and apoptosis assays. For cell cycle and apoptosis assays, both adherent and nonadherent cells were harvested, pooled, and fixed with 1% paraformaldehyde and 70% ethanol. For the cell cycle analysis, we stained cells with 50 μg/mL propidium iodide and determined the percentage of cells in specific cell cycle phases (G_1, S, and G_2-M) by using a flow cytometer equipped with a 488 nm argon laser (Epics Profile II; Beckman Coulter, Miami, FL). Approximately 1×10^4 cells were evaluated for each sample. Apoptosis was assessed with a flow cytometry–based terminal deoxyribonucleotide transferase–mediated nick-end labeling (TUNEL) assay processed with an APO-bromodeoxyuridine (APO-BrdUrd) staining kit (Phoenix Flow Systems, San Diego, CA); this assay was modified as previously described (25). Cells treated with DMSO were used as a negative control, and for a positive control, we used the HL-60 leukemic cells treated with camptothecin provided with the kit.

Establishment of resistant cell line. The H460 cell cultures were continuously exposed to erlotinib (10 μmol/L) in routine culture medium that was replaced every day for 5 months. Initially, H460 cell numbers were substantially reduced, and for the next 2 months, the surviving cells were passaged approximately every 10 days with a seeding ratio of 1:2. Cell proliferation slowly increased to allow a passage every 7 days with a seeding ratio of 1:4 over the next 2 months. A stable growth rate was reached after a total of 5 months with routine maintenance of the H460/TKI-R cells involving passage every 4 days with a seeding ratio of 1:8 of the confluent cell number.

Subcellular fractionation. The following procedures were done at 4°C. Cells were scraped into PBS [10 mmol/L sodium phosphate (pH 7.4) and 150 mmol/L NaCl] and then collected by centrifugation. Cell pellets were resuspended with 1 mL of hypotonic buffer [10 mmol/L Tris-HCl (pH 7.5), 1 mmol/L $MgCl_2$, 50 μg/mL leupeptin, 1 mmol/L phenylmethylsulfonyl fluoride, and 1 mmol/L Na_3VO_4]; 10 minutes later, the cells were transferred to a Dounce homogenizer and further disrupted by 25 strokes with a tight-fitting pestle. The homogenate was adjusted to the indicated NaCl concentration from a 5 mol/L stock solution, and nuclei were removed by centrifugation at 1,700 × *g* for 5 minutes. The postnuclear supernatant was centrifuged again at 10,000 rpm for 20 minutes to remove the mitochondrial fraction; the postmitochondrial supernatant was centrifuged at 45,000 × *g* for 60 minutes. The supernatant fraction, representing the cytosolic fraction, was adjusted to 1% NP40 from a 10% stock solution. The pellet, representing the plasma membrane fraction, was gently rinsed with 1 mL PBS and then resuspended in 1 mL hypotonic buffer containing 1% NP40.

Immunoblotting and coimmunoprecipitation. NSCLC cells (1×10^6 cells/100 mm^3 dish) were either left uninfected or infected with Ad-EV (50 pfu/cell) or Ad-survivin (50 pfu/cell) and then left untreated or treated with various concentrations of erlotinib (0.1-10.0 μmol/L), AG1024 (5.0 μmol/L), LY294002 (10.0 μmol/L), PD98059 (10.0 μmol/L), rapamycin (1.0 μmol/L), or their combinations in growth medium that was changed daily. When growth factor stimulation was done, cells were cultured in serum-free medium for 1 day and then incubated in EGF (50 ng/mL) or IGF (50 ng/mL) for 15 minutes. For the small interfering RNA (siRNA) transfection, H460 cells in the logarithmic growth phase in six-well plates (5×10^5 cells per well) were transfected with 10 μL of 20 μmol/L survivin siRNA or control scrambled siRNA (Dharmacon Research, Lafayette, CO) using LipofectAMINE 2000 (Invitrogen, Carlsbad, CA), according to the protocol of the manufacturer. After 24 hours of incubation in growth medium, erlotinib was added, and the cells were harvested after 3 days of incubation. Immunoprecipitations were done using 3 mg protein from the total cell lysates and 1 μg mouse monoclonal anti-EGFR antibody, mouse monoclonal anti-IGF-IR antibody (Oncogene Sciences, Uniondale, NY), or healthy preimmune serum anti-mouse for the negative control and by incubating overnight at 4°C. The immunocomplexes were precipitated with protein-G agarose (Pharmacia-LKB Biotechnology, Piscataway, NJ). The immunoprecipitates were resolved on 6% SDS-PAGE gels, followed by Western blotting as described elsewhere (25).

Metabolic labeling. Metabolic labeling was done with H460 and TKI-R cells (5×10^5 in six-well plates). Cells were washed in PBS and incubated in RPMI medium without methionine and cysteine (Sigma, St. Louis, MO) for 2 hours. Next, the medium was replaced with fresh medium containing methionine and cysteine, to final concentrations of 150 mg/L, and the cells were labeled with trans-^{35}S (0.5 mCi; ICN, MP Biomedicals, Irvine, CA). The cells were then treated with 0.1% DMSO or erlotinib (10 μmol/L) for 1, 3, 6, 12, and 24 hours. At harvesting time, the cells were washed in ice-cold PBS and lysed in radioimmunoprecipitation assay buffer. Lysates containing equal amounts of protein (100 μg) were immunoprecipitated using 1 μg of antibody to detect EGFR or 1 μg of antibody to detect survivin (both from Santa Cruz Biotechnology) and 30 μL of 50% slurry of protein G agarose beads (Pharmacia-LKB Biotechnology, Piscataway, NJ). The immunoprecipitates were washed five times with lysis buffer, separated by SDS-PAGE,

and analyzed autofluorographically. Cell extracts were also subjected to Western blot analysis for β-actin to ensure that equal amounts of protein had been used. Two independent experiments were done with similar results; representative results of one experiment are presented.

Northern blot analysis. H460 cells (1×10^6 in 10 mm^3 plates) were treated with erlotinib (10 μmol/L) for different times (0, 24, 48, and 72 hours). The total cellular RNA was isolated by the application of TRIzol. For the Northern blotting, 10 μg of the total cellular RNA prepared from each sample was subjected to electrophoresis on a 1% agarose gel containing 2% formaldehyde and then stained with ethidium bromide, photographed, transferred to a Z probe membrane (Bio-Rad Laboratories), and hybridized to an [α-^{32}P]dCTP-labeled EGFR cDNA probe.

***In vivo* model.** The effect of the combination of erlotinib and Ad-dnIGF-IR on established s.c. tumor nodules was studied in athymic nude mice (Harlan Sprague-Dawley) in a defined pathogen-free environment. Briefly, 6-week-old female nude mice were irradiated with 350 rad from a cesium-137 source and then were injected s.c. with 1×10^7 H1299 cells in 100 μL of growth medium at a single dorsal site. The mice were randomly assigned to one of four treatment groups, with each group containing eight mice. Group 1 (control mice) received 1× PBS and Ad-EV, group 2 received erlotinib and Ad-EV, group 3 received 1× PBS and Ad-dnIGF-IR, and group 4 received erlotinib and Ad-dnIGF-IR. Tumor growth was quantified by measuring the tumors in three dimensions with calipers for a total of 35 days. After the tumor volumes reached ~75 mm^3 (considered day 0), the mice were treated with p.o. administered erlotinib (100 mg/kg of body weight) twice a day. We chose this dosage of erlotinib because it had had no notable effect on H1299 tumor growth in preliminary experiments (data not shown). On day 23, when tumor volumes reached ~125 mm^3, each mouse was given a single intratumoral injection of 2×10^9 particles of Ad-dnIGF-IR or Ad-EV in 100 μL of PBS. Mice with necrotic tumors or tumors ≥1.5 cm in diameter were euthanized immediately. The results were expressed as the mean tumor volume ($n = 5$) with 95% confidence intervals (95% CI). On day 35, all mice were sacrificed and tumor tissues were collected from the xenografts to determine whether the combination of erlotinib and

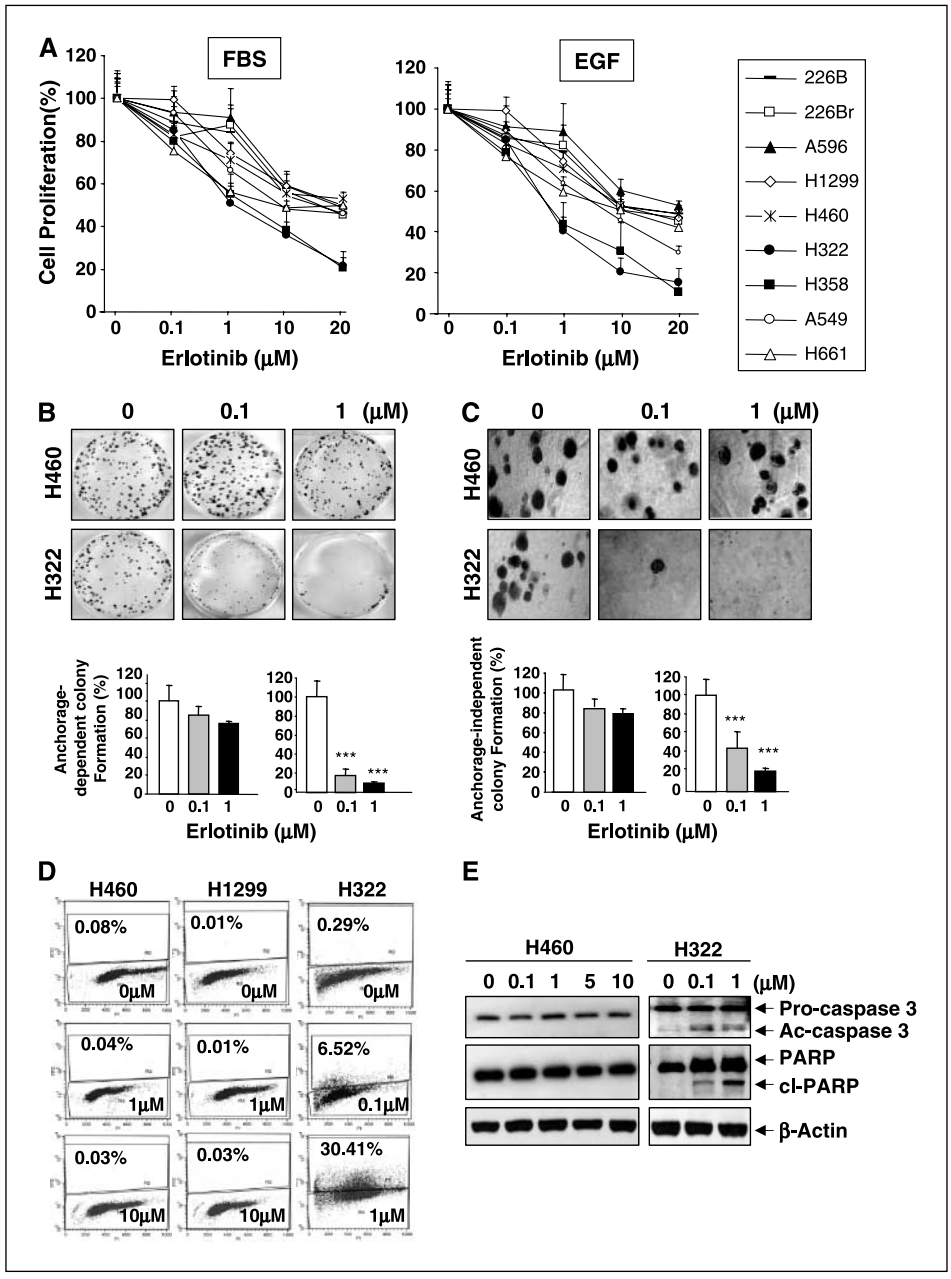

Figure 1. *A,* the MTT assay in NSCLC cell lines (H460, H1299, H661, A596, A549, H226B, H226Br, H322, and H358) treated with the indicated concentrations of erlotinib in RPMI 1640 containing 10% FBS or EGF for 3 days. *B,* clonogenic survival assay of H460 and H322 cells treated with the indicated concentrations of erlotinib. *C,* anchorage-independent growth assay of cells treated with the indicated concentrations of erlotinib. In (*A-C*), independent experiments were repeated thrice. *Columns,* mean of eight (*A*) or three (*B* and *C*) identical wells of a single representative experiment; *bars,* upper 95% CI; **, $P < 0.01$; ***, $P < 0.001$, for comparisons between erlotinib-treated and control cells. *D,* effects of the indicated concentrations of erlotinib on apoptosis in H322, H460, and H1299 NSCLC cells, assessed by a modified TUNEL assay. From a single representative experiment ($n = 2$). *E,* effects of the indicated concentrations of erlotinib on apoptosis-related enzyme expression in H322 and H460 NSCLC cells. The expression of caspase-3, PARP, and β-actin was assessed by Western blotting.

Ad-dnIGF-IR induced apoptosis *in vivo* by Western blot and immunohistochemical analyses as previously described (23).

Statistical analyses. The data acquired from the MTT assay were analyzed using Student's *t* test. All means and 95% CIs from eight samples were calculated using Microsoft Excel software (version 5.0; Microsoft Corporation, Seattle, WA). Cell survival comparisons among groups and statistical significance of differences in tumor growth in the combination treatment group and in the single-agent treatment groups were analyzed by ANOVA for 2×2 factorial design. All means from triplicate to eight samples and 95% CIs were calculated using SAS software (release 8.02; SAS Institute, Cary, NC). In all statistical analyses, two-sided *P* values of <0.05 were considered statistically significant.

Results

Differential apoptotic responses of NSCLC cells after treatment with erlotinib. To test the effects of EGFR TKIs on NSCLC cell proliferation, a subset of NSCLC cell lines (H460, H1299, H661, H596, H226B, H226Br, A549, H322, and H358) was treated with erlotinib in regular growth medium containing 10% FBS or in serum-free medium containing EGF. A MTT assay revealed that erlotinib has different levels of antiproliferative activities, depending on cell lines (Fig. 1*A*): Compared with the other NSCLC cell lines, H322 and H358 cells were more sensitive to the erlotinib treatment ($P < 0.001$). Approximately 1 μmol/L erlotinib significantly inhibited proliferation of H322 and H358 cells after 72 hours of treatment. In contrast, the drug concentrations required to inhibit cell growth by 50% for H460, H1299, H661, H596, H226B, H226Br, and A549 cells were 10 to 20 times higher than those needed to inhibit H322 and H358 cells. Consistent with the results from the MTT assay, erlotinib only slightly affected the anchorage-dependent and anchorage-independent colony-forming abilities of H460 and H1299 cells (data not shown) at concentrations <1 μmol/L, a concentration that significantly inhibited those abilities of H322 ($P < 0.001$; Fig. 1*B* and *C*; $P < 0.001$) and H358 (data not shown) cells.

We next asked whether the ability of 1 μmol/L erlotinib to inhibit H322 and H358 cell proliferation was due to decreased cell cycle progression and/or increased apoptosis. Flow cytometric analyses of propidium iodide–stained H460, H1299, and H322 cells revealed that treatment with 1 μmol/L erlotinib for 3 days resulted in no marked change in the cell cycle distribution (data not shown). However, fluorescence-activated cell sorter analysis followed by terminal deoxynucleotidyl transferase–mediated dUTP-biotin nick-end labeling (TUNEL) staining revealed induction of apoptosis in 30.4% of the H322 cells treated with 1 μmol/L erlotinib. In contrast, treatment with up to 10 μmol/L erlotinib did not detectably increase the apoptotic population of H1299 and H460 cells (Fig. 1*D*). In agreement with these findings, the protein levels of the active form of caspase-3 (Ac-caspase-3) and the cleaved form of poly(ADP-ribose) polymerase (PARP; cl-PARP, the 89 kDa fragment) increased in the H322 cells treated with >0.1 μmol/L erlotinib but not in the H460 cells, even after treatment with 10 μmol/L erlotinib (Fig. 1*E*). H358 cells also responded with apoptosis to similar concentrations of erlotinib (data not shown). Together, these findings indicated the presence of mechanisms that affect the response of NSCLC cells to erlotinib-mediated apoptosis.

Role of IGF-IR signaling pathways in the development of resistance to erlotinib treatment in NSCLC cells. To investigate the mechanisms involved in the sensitivity of NSCLC cells to erlotinib, we first tested whether erlotinib successfully blocks activation of EGFR and its downstream mediators in NSCLC cell lines. Figure 2*A* shows that 0.1 to 1.0 μmol/L erlotinib suppressed the levels of phosphorylated EGFR (pEGFR), phosphorylated Akt (pAkt), and phosphorylated p44/42 MAPK (pp44/42 MAPK) in H460 and H1299 cells (cell lines that are weakly sensitive to erlotinib) and H322 and H358 cells (cell lines that are very sensitive to the drug). However, comparable induction of pAkt and p44/42 MAPK was evident in H460 and H1299 cells after treatment with >5.0 μmol/L erlotinib, doses that induce apoptosis in most of the H322 and H358 cells. pAkt and p44/42 MAPK are located in the nodal points of growth factor–mediated cell survival signaling, and the IGF-IR pathway can modulate the action of the erbB family blocking agents in various cancer cells (25–27). Hence, we tested whether IGF-IR was involved in increases in pAkt and p44/42 MAPK. Indeed, erlotinib concentrations >5.0 μmol/L induced phosphorylated IGF-IR (pIGF-IR) in H460 and H1299 cells but not in H322 and H358 cells.

We then studied the influence of IGF-IR signaling pathways on the response of NSCLC cells to erlotinib. H460 cells exhibited significantly decreased proliferation and anchorage-dependent and anchorage-independent colony-forming abilities when the cells were treated with erlotinib in serum-free medium compared with when they were treated in the presence of IGF-I. H322 cells, however, showed statistically significant sensitivity to erlotinib in all conditions (Fig. 2*B*), suggesting that the induced activation of the IGF-IR signaling pathway allows NSCLC cells to survive and proliferate when the EGFR pathway is blocked by erlotinib treatment.

To test our hypothesis, we compare the effects of erlotinib, either single or in combination with AG1024, an IGF-IR TKI, on the proliferation, clonogenic survival ability, and apoptosis of H460 cells. AG1024 has shown significantly lower affinity for the insulin receptor than for the IGF-IR (26). Combined treatment with erlotinib and AG1024 synergistically enhanced the antiproliferative effects of erlotinib on H460 cells compared with single treatment with each drug when cultured in complete (FBS) or serum-free medium in the absence or presence of IGF ($P < 0.001$; Fig. 2*C*; Supplementary Table S1). Erlotinib also showed significantly enhanced antiproliferative properties in H460 cells infected with an Ad-dnIGF-IR compared with the control cells infected with Ad-EV ($P < 0.001$; Fig. 2*D*). Moreover, combined treatment with erlotinib and AG1024 (Fig. 2*E*) or Ad-dnIGF-IR (Fig. 2*F*) significantly suppressed the anchorage-dependent, colony-forming ability of H460 cells ($P < 0.001$; Supplementary Table S2). Furthermore, TUNEL staining and flow cytometric analysis revealed that ~1% of control H460 cells, 1.2% of erlotinib-treated cells, and 26% (95% CI, 14.3-37.6%, $P < 0.05$) of AG1024-treated cells underwent apoptosis. In contrast, combined treatment with both erlotinib and AG1024 significantly enhanced TUNEL staining (77.1%; 95% CI, 64.4-89.8%; $P < 0.001$; Fig. 2*G*) and induced cleavage of the 113-kDa PARP to the 89-kDa fragment in parallel with the concomitant decreases in the levels of pIGF-IR, pAkt, and p44/42 MAPK (Fig. 2*H*). These findings suggest that the IGF-IR pathway provides an alternative proliferation and/or survival mechanism for NSCLC cancer cells in which EGFR is blocked by erlotinib.

Evidence of increased heterodimerization and membrane localization of IGF-IR and EGFR in erlotinib-treated H460 cells. We investigated the mechanism underlying NSCLC cell resistance to erlotinib using *in vitro* model of the H460 cell line (H460/TKI-R) that had been continuously treated with erlotinib. Treatment with >10 μmol/L erlotinib decreased the number of H460 cells, but proliferation of the remaining cells gradually

increased after 3 months of erlotinib treatment. Compared with the parent H460 cells, the H460 cells treated with 10 μmol/L erlotinib for 5 months (H460/TKI-R) had higher levels of pIGF-IR, pAkt, and pp44/42MAPK, with no detectable differences in the expression of IGF-IR, Akt, and p44/42MAPK (Fig. 3*A*). The dose-response curves in Fig. 3*B* revealed no detectable cytotoxicity from erlotinib treatment of the H460/TKI-R cells up to a concentration of 20 μmol/L, whereas inhibition of IGF-IR activation by the AG1024 treatment induced greater antiproliferative effects on the H460/TKI-R cells than it did on the H460 cells. Moreover, compared with a single agent, combined treatment with erlotinib and AG1024 significantly suppressed the anchorage-dependent, colony-forming ability of H460/TKI-R as well as H460 cells ($P < 0.001$; Fig. 3*C*). The effects of combined treatment with erlotinib and AG1024 on colony formation was greater in H460/TKI-R cells than in H460 cells, indicating the dependence of H460/TKI-R cells on the IGF-IR signaling pathway for maintaining cell proliferation and tumorigenic potential.

We investigated the mechanism of erlotinib-mediated activation of IGF-IR in H460 cells. One mechanism by which the growth factor receptor is activated in tumor cells is by receptor dimerization; another is by overwhelming negative regulatory mechanisms that suppress receptor activation. Recent studies have revealed the interaction between the ErbB receptor families and IGF-IR in several tumor models, including breast cancer and oral cancer cell lines (19, 28–32). We, therefore, tested whether EGFR interacts with IGF-IR in H460/TKI-R cells by performing immunoprecipitation. EGFR immunoprecipitates from H460/TKI-R cells showed greater IGF-IR binding compared with that from the parental H460 cells (Fig. 3*D*). Control immunoprecipitates using preimmune serum exhibited no immunoreactive band. The interaction between EGFR and IGF-IR was observed as early as 30 minutes after the erlotinib treatment (Fig. 3*E*). In contrast, no detectable change was observed in the levels of EGFR-EGFR or EGFR-ErbB2 interaction in H460 cells treated with erlotinib for 3 days (Fig. 3*F, top*). Similarly, IGF-IR immunoprecipitates from erlotinib-treated H460 cells showed greater levels of EGFR binding than untreated cells did (Fig. 3*F, bottom*), whereas no detectable binding was observed when the IGF-IR immunoprecipitates were immunoblotted to ErbB2 or ErbB3. Increased EGFR/IGF-IR heterodimerization was also observed in H1299 cells treated with 10 μmol/L erlotinib (Fig. 3*G*). In contrast, the EGFR and control (preimmune serum) immunoprecipitates from untreated or erlotinib-treated H322 cells exhibited no immunoreactive band. These results suggested that erlotinib induces physical contact between EGFR and IGF-IR, which is accumulative.

Erlotinib treatment–induced expression of survivin protein protects NSCLC cells from apoptosis. We next attempted to find evidence connecting erlotinib-induced activation of the IGF-IR with survival of NSCLC cells. Because the inhibitor of apoptosis

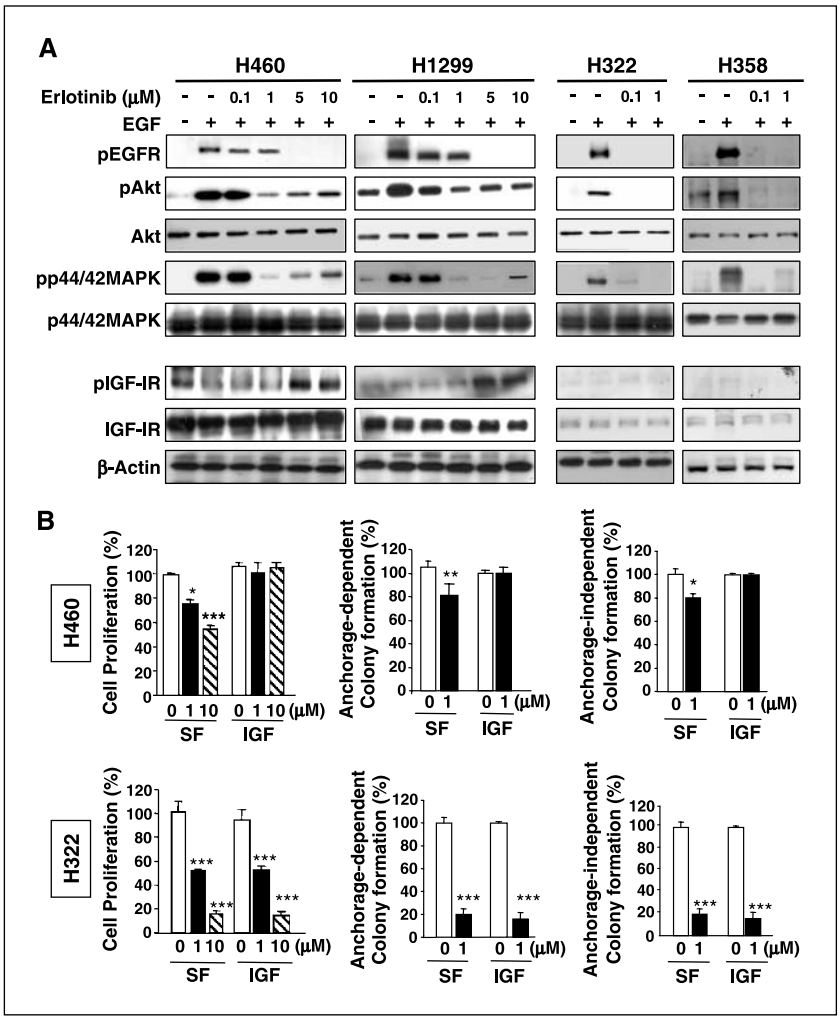

Figure 2. *A,* immunoblotting of the EGFR, IGF-IR, and their downstream signaling components in NSCLC cells treated with indicated concentrations of erlotinib. Western blotting on β-actin is included as a loading control. *B,* role of the IGF-I on the proliferation and survival of NSCLC cells. *Left,* MTT assay in H460 and H322 cells incubated in the serum-free medium without (*SF*) or with IGF-I (50 ng/mL) in the presence of indicated concentrations of erlotinib for 3 days. *Middle* and *right,* efficacy of the indicated concentrations of erlotinib in inhibiting anchorage-dependent and anchorage-independent growth of H460 and H322 cells, respectively, in serum-free and IGF-dependent conditions.

proteins, including survivin and XIAP, decrease the sensitivity of tumor cells to chemotherapeutic drugs, thereby conferring resistance to apoptosis (21, 33), we tested the effects of erlotinib on the expression of these proteins in a subset of NSCLC cells with weak or great sensitivity to erlotinib. We found that expression of survivin but not XIAP markedly increased in H1299, H460, H661, A549, A596, and 226B cells (Fig. 4*A, top*) during the time IGF-IR was phosphorylated by the erlotinib treatment (Fig. 4*A, bottom*). In contrast, H358 and H322 cells showed no detectable changes in the protein levels of survivin, XIAP, and pIGF-IR during the time EGFR was inactivated by erlotinib treatment. Erlotinib induced survivin expression in a time- and dose-dependent manner (Fig. 4*B*). Interestingly, a similar but less pronounced increase in EGFR expression was observed in H1299, H460, H661, A549, H596 H226Br, and H226B, H460/TKI-R cells but not in H358 and H322 cells. Increases in the survivin and EGFR expression were also observed in H460/TKI-R cells (Fig. 4*C*).

We then tested the response of H460 cells, in which survivin expression was abolished by siRNA transfection. Western blot analysis revealed an obvious increase in PARP cleavage in the 460 cells by the treatment with erlotinib (Fig. 4*D*). Among H322 cells, in which survivin overexpression was induced by the infection with Ad-survivin, the PARP cleavage was substantially reduced after the erlotinib treatment (Fig. 4*E*). These results indicated that increased expression of survivin protein protected NSCLC cells from the erlotinib-induced apoptosis.

mTOR pathway induces *de novo* protein synthesis of EGFR and survivin and protects NSCLC cells from apoptosis. We investigated the mechanisms of erlotinib-mediated increase in survivin and EGFR protein expression. According to Northern blot analysis, exposure of H460 cells to erlotinib resulted in no change in the mRNA levels of survivin (Fig. 5*A*) and EGFR (data not shown). We then determined the effects of erlotinib on the rates of survivin and EGFR protein synthesis. Metabolic labeling of the H460 cells with [^{35}S]Met-Cys revealed that the rate of [^{35}S]labeled survivin (Fig. 5*B*) and EGFR (data not shown) synthesis was remarkably greater in the erlotinib-treated H460 and H460/TKI-R cells than in the untreated parental H460 cells. We then determined whether

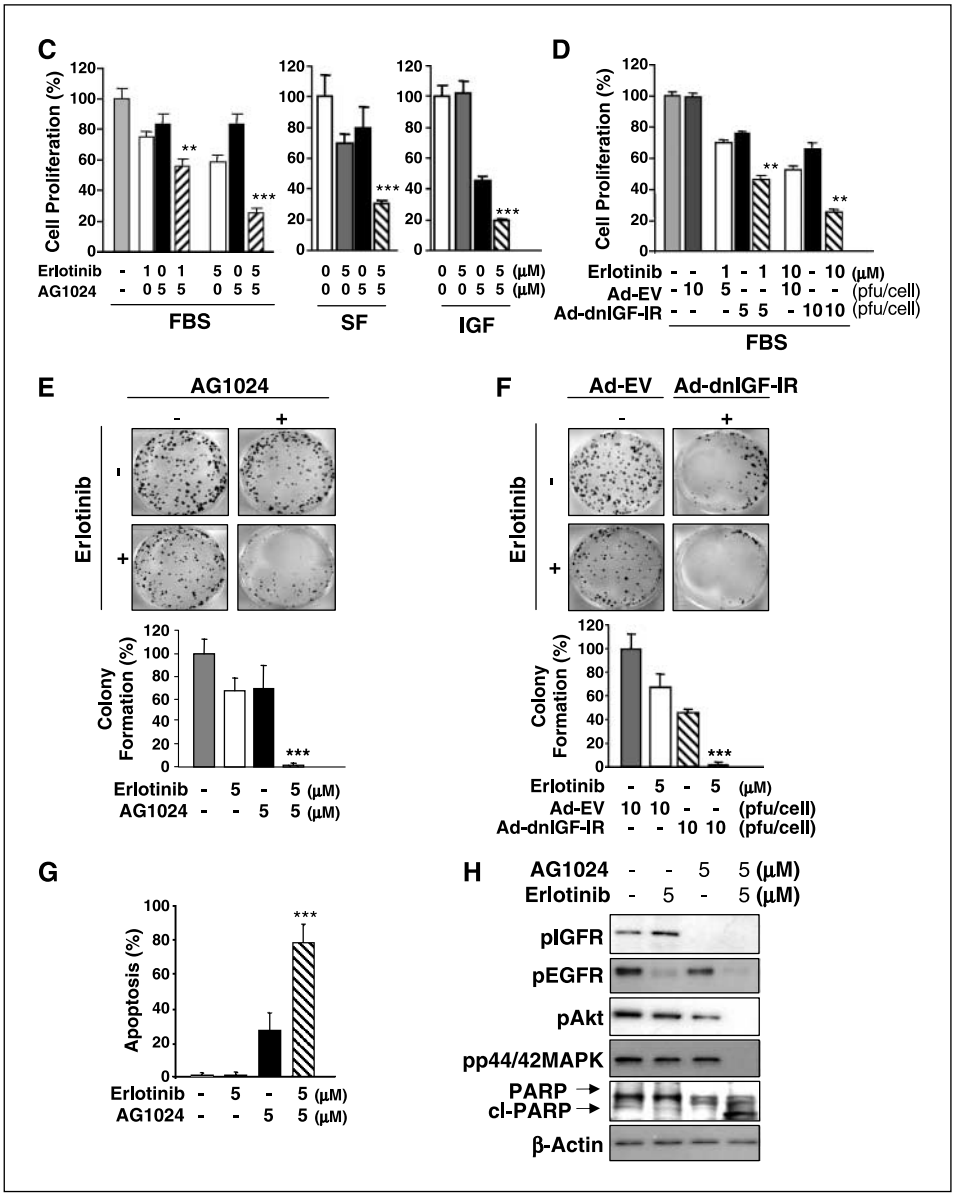

Figure 2 *Continued.* *C* and *D,* effect of targeting both the EGFR and the IGFR-IR on cell proliferation. MTT assay in H460 cells uninfected (*C*) or infected with 5 or 10 infectious forming unit of Ad-EV or Ad-dnIGF-IR (*D*) and treated with indicated concentrations of erlotinib, AG1024, or their combination in serum-free RPMI 1640 containing 10% FBS or IGF (50 ng/mL) for 3 days. *E* and *F,* survival of H460 cells treated with erlotinib (5 μmol/L), AG1024 (5 μmol/L), or their combination (*E*), or cells infected with 10 pfu/cell of Ad-EV or Ad-dnIGF-IR and then untreated or treated with erlotinib (5 μmol/L; *F*) were assessed by counting colonies consisting of >50 cells after 10 days of growth. *G* and *H,* effects of 5 μmol/L erlotinib, 5 μmol/L AG1024, or their combination on apoptosis (*G*) and expression of pEGFR, pIGF-IR, pp44/42MAPK, and pAkt (*H*) were analyzed in H460 cells by a flow cytometry–based TUNEL assay and Western blotting. β-Actin, loading control. *Columns,* mean value of eight (MTT) or three (clonogenic growth assay and TUNEL assay) identical wells of a single representative experiment ($n = 3$); *bars,* upper 95% CI (*B-G*). ***, $P < 0.001$ for comparisons between cells treated with drug combination and cells treated with single agent.

mTOR is involved in the erlotinib-induced protein synthesis of survivin and EGFR by determining the levels of phosphorylated 4E-BP1 and $p70^{s6k}$, downstream mediators of mTOR (27, 34), in the H460 cells treated with erlotinib alone or in combination with rapamycin, an mTOR inhibitor, or AG1024 for 3 days. Western blot analysis revealed that erlotinib up-regulated the protein levels of p4E-BP1, $pp70^{s6k}$ in association with increases in survivin and EGFR expression, all of which were suppressed by

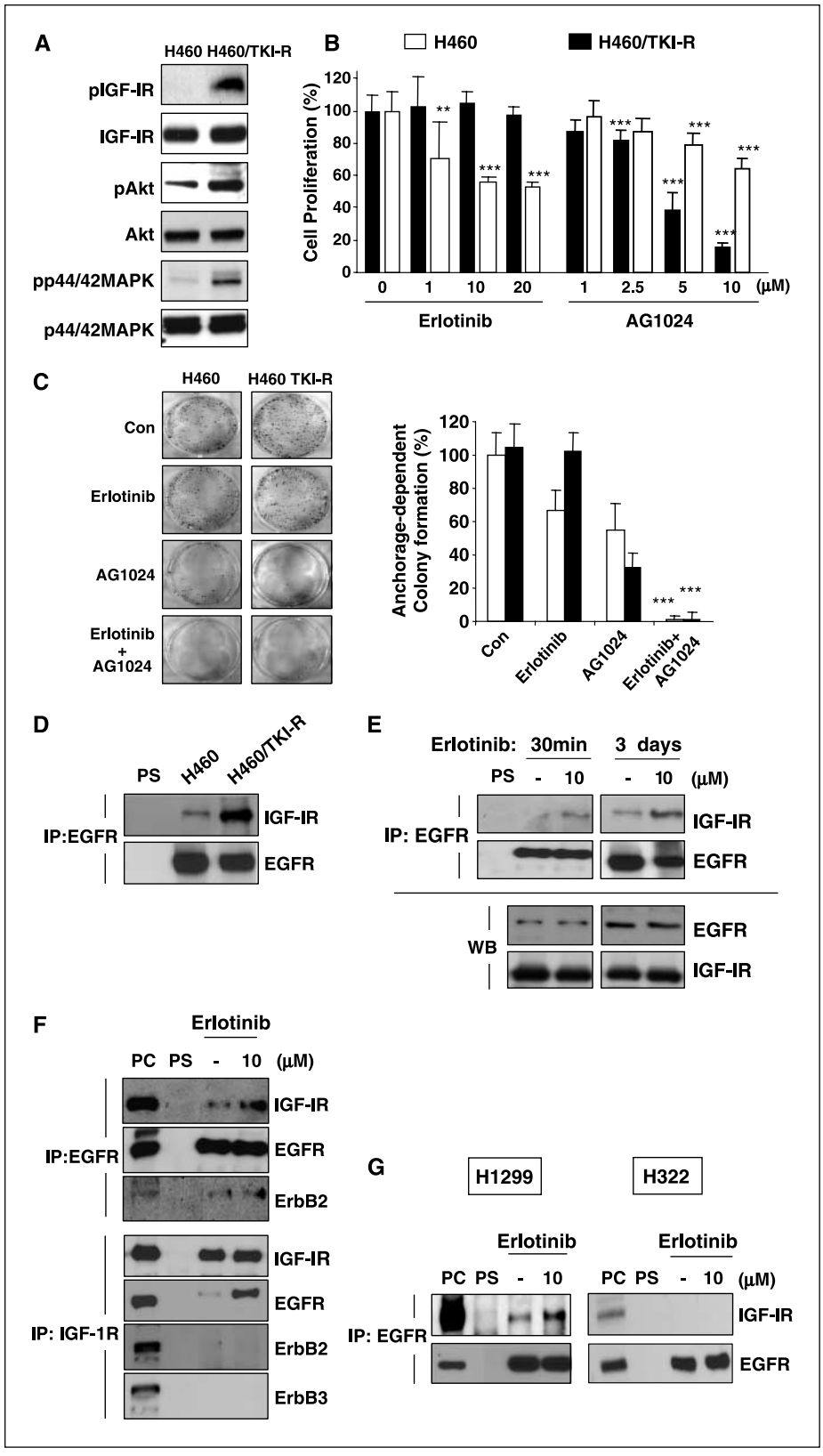

Figure 3. *A,* Western blot analysis of indicated protein expressions in H460 and H460/TKI-resistant (H460/TKI-R) cells. *B,* MTT assay on the proliferation of H460 and H460/TKI-R cells treated with erlotinib (1-20 μmol/L) or AG1024 (1-10 μmol/L). Cells treated with 0.1% DMSO were included as a control (0). *C,* survival of H460 and H460/TKI-R cells treated with erlotinib (5 μmol/L), AG1024 (5 μmol/L), or their combination. *Columns,* mean value of eight (MTT) or three (clonogenic assay) identical wells of a single representative experiment ($n = 3$); *bars,* upper 95% CI (*A* and *B*). ***, $P < 0.001$ compared with control. *D* to *G,* coimmunoprecipitation was done for the interaction between EGFR and IGF-IR. Whole-cell extracts from H460 and H460/TKI-R cells (*D*) or H460 cells, H1299, and H322 cells untreated or treated with erlotinib (10 μmol/L) for 30 minutes (*E*) or 3 days (*E-G*) were immunoprecipitated (*IP*) with anti-EGFR or anti-IGF-IR antibodies. The immunoprecipitates were subjected to Western blot analysis with indicated antibodies. Input (*PC*) represents cell lysates that were not subjected to immunoprecipitation. Control immunoprecipitation was done using control mouse preimmune serum (*PS*).

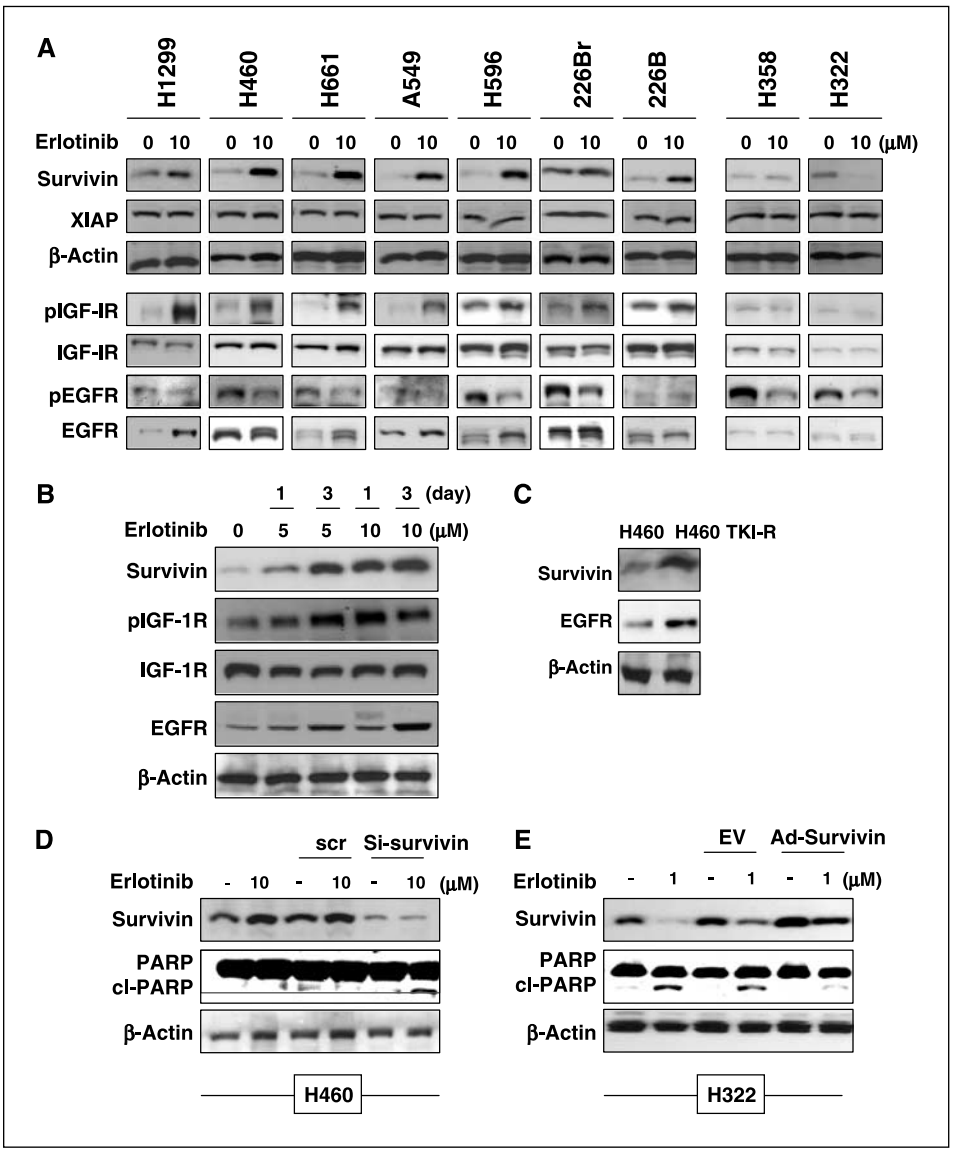

Figure 4. *A* and *B,* Western blot analysis on the survivin, XIAP, pIGF-IR, IGF-IR, pEGFR, EGFR protein expression in indicated NSCLC cell lines treated with erlotinib (1-10 μmol/L) for 1 (*B*) or 3 (*A, B*) days. *C,* Western blot analysis on the survivin and EGFR protein in H460 TKI/R cells. *D,* effect of the knockdown of survivin expression on H460 cells in the presence of erlotinib. H460 cells transfected with scramble (*scr*) or survivin siRNA (*si-survivin*), untreated and treated for 48 hours with erlotinib (10 μmol/L), were subjected to protein extraction and Western blotting for evaluation of caspase-3 (pro-caspase-3) and PARP. Loading control: β-actin. *E,* effects of overexpression of survivin in erlotinib-induced apoptosis in H322 cells. H322 cells were infected with 50 pfu/cell of control virus (Ad-EV) or Ad-survivin and incubated for 3 days in the presence of erlotinib (1 μmol/L). Protein extract was subjected to Western blotting for evaluation of survivin, caspase-3 (pro-caspase-3), and PARP. Loading control: β-actin.

treatment with AG1024 or rapamycin (Fig. 5*C*). Moreover, the combined treatment with AG1024, LY294002 (PI3K inhibitor), PD98059 (MEK inhibitor), or rapamycin reduced the levels of membranous EGFR expression (Fig. 5*D*) and of the EGFR and IGF-IR heterodimer (Fig. 5*E*) induced by the 3 days treatment of erlotinib. These findings suggested that the increases in the levels of EGFR/IGF-IR heterodimer on cell membrane and protein expressions of survivin and EGFR were mediated at least in part through translation-dependent events mediated by IGF-IR signaling pathways. We then tested whether inhibitors of the IGF-IR and mTOR pathways sensitize the H460 cells to the erlotinib treatment. H460 cells treated with erlotinib and AG1024 (Fig. 2*G* and *H*) or rapamycin (Fig. 5*F*) showed an increase in the PARP cleavage, suggesting that suppression of IGF-IR and mTOR pathways could restore the apoptotic activities of erlotinib in NSCLC cells.

Antitumor efficacy of dual targeting of EGFR and IGF-IR signaling pathways *in vivo*. To determine whether the inhibition of IGF-IR signaling can enhance the antitumor activities of erlotinib *in vivo*, we tested the effects of erlotinib, Ad-dnIGF-IR, and their combination on the growth of H1299 NSCLC xenograft tumors established in athymic nude mice. The mice treated with erlotinib plus Ad-dnIGF-IR showed synergistically reduced tumor growth compared with the control mice or the mice treated with erlotinib or Ad-dnIGF-IR alone (Fig. 6*A*; Supplementary Table S3). At the end of the study, the mean tumor volume in combined treatment group was 23% ($P < 0.001$) of the mean volume in the control group. Thus, the combination of erlotinib and Ad-dnIGF-IR enhanced the antitumor effects on the growth of NSCLC cells *in vivo*.

We then determined the effects of erlotinib, Ad-dnIGF-IR, and their combination on the activation of the IGF-IR and EGFR, the expression of survivin and EGFR, and the induction of apoptosis *in vivo*. According to Western blot analysis of total protein extracts harvested from the H1299 xenograft tumor tissues, the levels of pEGFR were decreased by erlotinib. In addition, erlotinib treatment induced marked increases in the levels of pIGF-IR, EGFR, and survivin, all of which were effectively blocked by Ad-dnIGF-IR (Fig. 6*B*). Combined treatment with erlotinib and Ad-dnIGF-IR also increased the levels of Ac-caspase-3, which is confirmed by the

immunohistochemical staining of the H1299 xenograft tumor tissues (Fig. 6*C*). Together, these findings suggested that the combined treatment with erlotinib and Ad-dnIGF-IR exert enhanced *in vivo* antitumor activities by decreased expression of survivin and EGFR and induction of apoptosis.

Discussion

Several preclinical and clinical discoveries have associated EGFR TKIs with antitumor activities. However, the limited response rates of patients to EGFR TKIs, even in patients with high levels of EGFR (15, 16, 35), have been raising questions about the mechanisms leading to the EGFR TKI resistance. Although somatic mutations of the EGFR ATP binding site have been associated with the response to the EGFR TKIs in some cases (17, 18), increasing number of evidence have suggested that the presence of other pathways that mediate the resistance of cancer cells to EGFR TKI therapy (36, 37). In this article, we have shown, to our knowledge for the first time, that erlotinib induces survival of NSCLC cells by inducing heterodimerization of EGFR/IGF-IR, activating IGF-IR pathway and its downstream mediators Akt and p44/42 MAPK, and thus stimulating mTOR-mediated protein synthesis of survivin that plays a crucial role in the blocking apoptosis. We showed here that the blockade of the IGF-IR to mTOR signaling pathway was sufficient to suppress *de novo* survivin protein synthesis and to restore apoptotic activities of erlotinib in NSCLC cells *in vitro* and *in vivo*. Our data present clear evidence that crosstalk between the IGF-IR and the EGFR signaling pathways and consequential survivin expression are involved in the NSCLC cell resistance to erlotinib. The erbB2/Her2/neu, a known preferred coreceptor for the EGFR, has been suggested to play a role in inducing NSCLC cell survival against EGFR TKIs (28). However, we found that the erbB2/Her2/neu was inactivated by the EGFR TKIs in NSCLC cells (data not shown), consistent with previous reports (38). In addition, an interaction between IGF-IR and erbB2 was undetectable, regardless of erlotinib treatment. Therefore, erbB2/Her2/neu is not likely to have a role in inducing EGFR TKI resistance in NSCLC cells.

We investigated the detailed mechanism that mediates IGF-IR activation by erlotinib and the consequent development of drug resistance. Given that gefitinib-resistant DU145/TKI-R prostate cells have shown considerably higher basal levels of IGF-II mRNA than wild-type cells (19), erlotinib might have increased the expression of IGF and conferred resistance to the drug to NSCLC cells. However, in gefitinib-resistant breast cancer cell lines, the IGF II mRNA level did not differ from that of the original clone (19), indicating that autocrine/paracrine production is not entirely responsible for the sensitivity of the cell to EGFR TKIs. Perhaps our most striking finding was that in H460 and H1299 cells, erlotinib induced heterodimerization between IGF-IR and EGFR. The interaction between EGFR and IGF-IR also has been observed in cancer cells (29–31). Given the considerable similarity between EGFR and IGF-IR in the sequence of their extracellular domain (39) and their reliance on EGF and IGF to achieve cell cycle progression and survival, it is plausible that erlotinib-mediated IGF-IR/EGFR heterodimerization can stimulate intracellular signaling components in a distinct pattern and allow NSCLC cells to resist the drug.

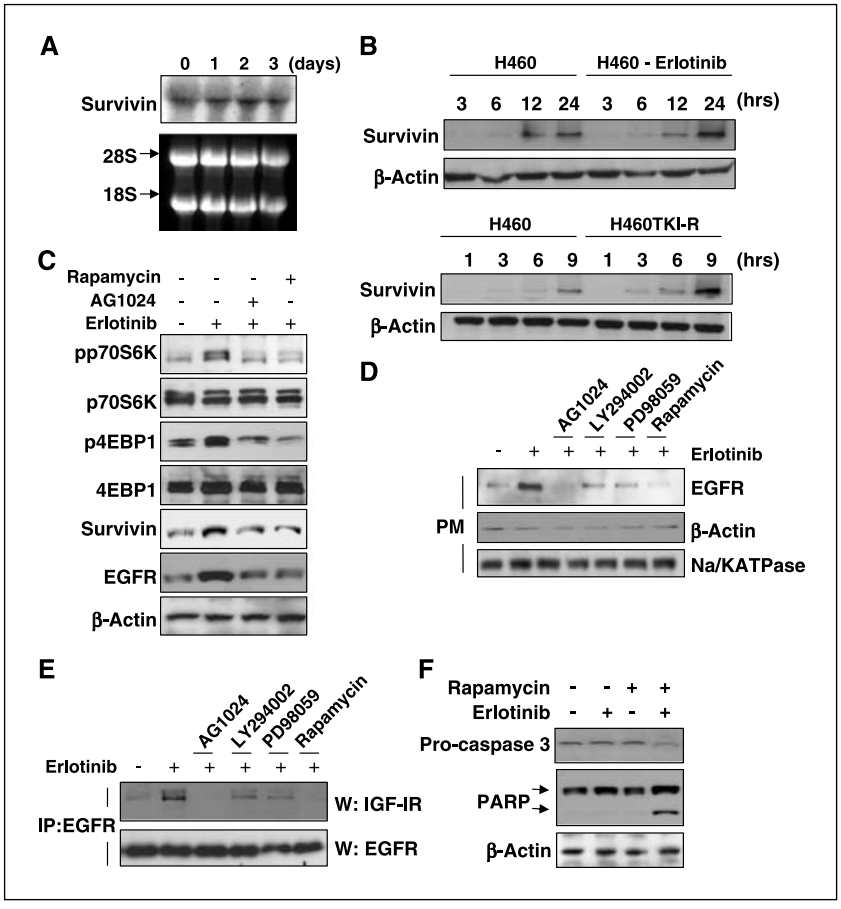

Figure 5. *A,* Northern blot analysis on survivin mRNA in H460 treated with erlotinib (10 μmol/L) for 1, 2, or 3 days. *B,* survivin and EGFR protein synthesis evaluated by metabolic labeling in untreated 460 cells, H460 cells treated with erlotinib (10 μmol/L), and H460TKI-R cells. Cell extracts were also subjected to Western blot analysis for β-actin to ensure that equal amounts of protein were used. *C,* expression of phosphorylated p70S6K (pp70S6k), p70S6K, phosphorylated 4EBP1 (p4EBP1), 4EBP1, survivin and EGFR in H460 cells treated with erlotinib (10 μmol/L), either single or in combination with AG1024 (5 μmol/L) or rapamycin (1 μmol/L), for 3 days. *D* and *E,* effects of erlotinib in combination with AG1024, LY294002, PD98059, or rapamycin on the plasma membrane (*PM*) localization of EGFR (*D*) and on the interaction between EGFR and IGF-IR (*E*). β-Actin, control for cytosol fraction; Na/K ATPase, control for plasma membrane fraction. *F,* effect of combined treatment with erlotinib (10 μmol/L) and rapamycin (1 μmol/L) for 3 days on apoptosis in H460 cells. Protein extract was subjected to Western blotting for the evaluation of pro-caspase-3 and PARP. Loading control: β-actin.

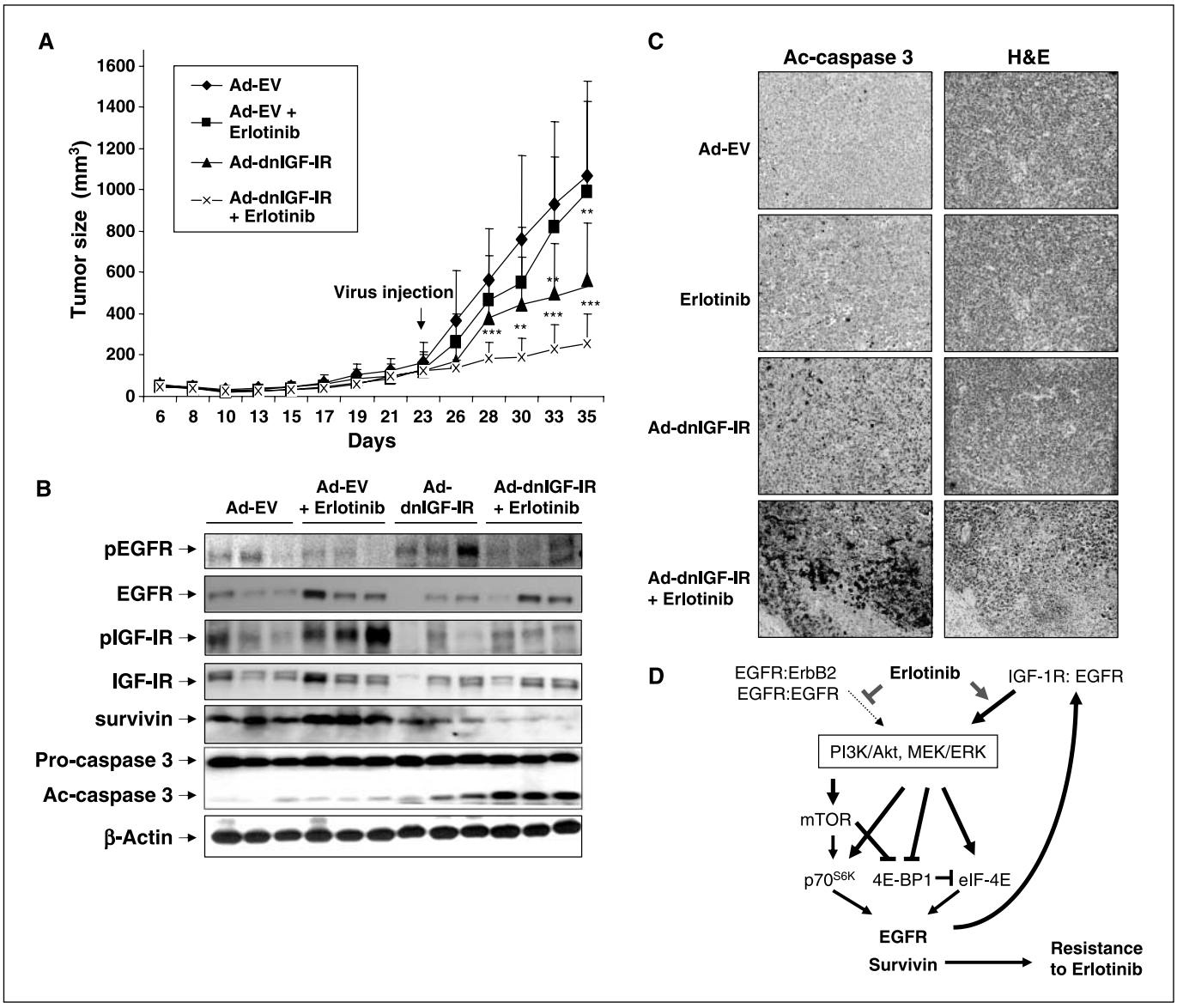

Figure 6. Effects of combined treatment with erlotinib and recombinant Ad-dnIGF-IR on growth of H1299 NSCLC xenograft tumors in athymic nude mice. The mice were randomly assigned to one of four treatment groups, with each group containing five mice. Group 1 (control mice) received 1× PBS and Ad-EV, group 2 received erlotinib and Ad-EV, group 3 received 1× PBS and Ad-dnIGF-IR, and group 4 received erlotinib and Ad-dnIGF-IR. *A,* effect of erlotinib (40 mg/kg body weight, administered p.o. twice daily) on tumor volume. When tumor volume was ~125 mm^3, mice were treated with Ad-IGF-IR or Ad-EV (control) in 100 μL PBS. *Points,* mean tumor volume (n = 5) with 95% CI; *bars,* SE. **, $P < 0.01$, ***, $P < 0.001$ for comparisons between drug-treated and control cells for each series of experiments. *B,* effects of erlotinib and Ad-dnIGF-IR on the expression of pEGFR, EGFR, pIGF-IR, IGF-IR, survivin, and pro-caspase-3 and Ac-caspase-3 in NSCLC xenograft tumors, assessed by Western blotting. β-Actin = loading control. *C,* effects of combined erlotinib and Ad-IGF-IR on expression of Ac-caspase-3. Tissues were stained with H&E. Representative section from each condition. *D,* schematic model of resistance mechanism to erlotinib.

Previous studies have shown the ability of erlotinib to induce EGFR mRNA and protein expression in the erlotinib-resistant biliary tract cancer cell line HuCCT1 but not in the susceptible A431 epidermoid cell line (40). In current study, we found that erlotinib induces mTOR-mediated *de novo* protein synthesis of survivin and EGFR with no detectable change in their mRNA levels, indicating diverse responses of different cancer cells to erlotinib. Our results may explain some apparently paradoxical findings in several clinical trials (41), in which up-regulation of pEGFR was observed after treatment of breast cancer patients with erlotinib. In another report, modifications of EGFR serum values during treatment of NSCLC seemed to reflect gefitinib activity; responding patients showed decreased serum levels of EGFR relative to those in patients with refractory disease (42). Our data also show the critical role of the induced survivin proteins in the development of resistance to erlotinib; (*a*) survivin expression was induced in NSCLC cell lines with weak sensitivity to the erlotinib treatment; (*b*) overexpression of survivin protected the sensitive NSCLC cells from erlotinib-induced apoptosis; and (*c*) knockdown survivin expression by siRNA provoked apoptosis in NSCLC cells with weak erlotinib sensitivity. mTOR has been known to regulate the translation of subsets of mRNA, many of which encode for proteins involved with driving cell growth, proliferation, and angiogenesis (43). Therefore, resistance and sensitivity to erlotinib in NSCLC may be determined at least in part by the ability of the cancer cells to stimulate mTOR-mediated synthesis of specific proteins that

have key roles in cell proliferation and/or survival and thus to adapt to a stressful environment.

In summary, our findings provide definitive *in vitro* and *in vivo* evidence that erlotinib induces heterodimerization of the EGFR/IGF-IR and stimulates IGF-IR and downstream pathways, including PI3K/Akt, MEK/extracellular signal-regulated kinase (ERK), resulting in the mTOR-mediated increases in EGFR and survivin proteins. On the basis of these findings, it is plausible to suggest that increased EGFR proteins further enhance the interplay between the EGFR and IGFR on the cell membrane, resulting in a further amplification of IGF-IR to mTOR signaling. In addition, the increased survivin proteins seem to provide survival potential to the NSCLC cells against the erlotinib treatment (Fig. 6*D*).

Our findings have direct effect to the treatment of NSCLC with erlotinib. The data showing no detectable interaction between EGFR/IGF-IR in NSCLC cell lines with low levels of IGF-IR expression suggests that the expression of IGF-IR is an important factor for the EGFR and IGF-IR complex and erlotinib sensitivity. Therefore, IGF-IR expression may serve as a predictor for erlotinib resistance in NSCLC. IGF-IR signaling pathway also plays a key role in the resistance to several therapeutic drugs (12, 27, 44–47). Overexpression of IGF-IR has been observed in various human cancers, including lung cancer (48), and is associated with a poor prognosis (49). Importantly, our unpublished data showed that clinical samples from NSCLC patients revealed that the majority of EGFR-overexpressing samples showed correlative increases in IGF-IR protein levels compared with their paired normal counterparts from the same patients. With this prospect, IGF-IR–targeting combination treatment may be required when erlotinib is considered as a therapeutic agent for NSCLC patients. Alternatively, mTOR inhibitors could confer benefit to erlotinib-resistant patients. In light of this notion, we have shown that combined treatment with erlotinib and inhibitors of IGF-IR or mTOR suppressed survivin and EGFR expression, decreased proliferation of NSCLC cells, and induced apoptosis in NSCLC cells *in vitro* and *in vivo*. Further studies are warranted to validate whether the erlotinib combined with inhibitors of IGF-IR or mTOR inhibitors could enhance the objective response and survival rates in NSCLC patients.

Acknowledgments

Received 5/10/2006; revised 7/6/2006; accepted 8/22/2006.

Grant support: NIH grant R01 CA100816 (H-Y. Lee), American Cancer Society grant RSG-04-082-01-TBE 01 (H-Y. Lee), Department of Defense grants W81XWH-04-1-0142-01-VITAL and W81XWH-06-1-0303-BATTLE, and partly by The National Foundation for Cancer Research Fellow grants (W.K. Hong).

The costs of publication of this article were defrayed in part by the payment of page charges. This article must therefore be hereby marked *advertisement* in accordance with 18 U.S.C. Section 1734 solely to indicate this fact.

References

1. Jemal A, Murray T, Samuels A, Ghafoor A, Ward E, Thun MJ. Cancer statistics, 2003. CA Cancer J Clin 2003; 53:5–26.
2. Ferreira CG, Huisman C, Giaccone G. Novel approaches to the treatment of non-small cell lung cancer. Crit Rev Oncol Hematol 2002;41:57–77.
3. Mendelsohn J. The epidermal growth factor receptor as a target for cancer therapy. Endocr Relat Cancer 2001; 8:3–9.
4. Brognard J, Clark AS, Ni Y, Dennis PA. Akt/protein kinase B is constitutively active in non-small cell lung cancer cells and promotes cellular survival and resistance to chemotherapy and radiation. Cancer Res 2001;61:3986–97.
5. Brognard J, Dennis PA. Variable apoptotic response of NSCLC cells to inhibition of the MEK/ERK pathway by small molecules or dominant negative mutants. Cell Death Differ 2002;9:893–904.
6. Khazaie K, Schirrmacher V, Lichtner RB. EGF receptor in neoplasia and metastasis. Cancer Metastasis Rev 1993;12:255–74.
7. Ellerbroek SM, Halbleib JM, Benavidez M, et al. Phosphatidylinositol 3-kinase activity in epidermal growth factor-stimulated matrix metalloproteinase-9 production and cell surface association. Cancer Res 2001;61:1855–61.
8. Sandler A. Clinical experience with the HER1/EGFR tyrosine kinase inhibitor erlotinib. Oncology (Huntingt) 2003;17:17–22.
9. Ready N. Inhibition of the epidermal growth factor receptor in combined modality treatment for locally advanced non-small cell lung cancer. Semin Oncol 2005; 32:S35–41.
10. Hidalgo M. Erlotinib: preclinical investigations. Oncology (Huntingt) 2003;17:11–6.
11. Moyer JD, Barbacci EG, Iwata KK, et al. Induction of apoptosis and cell cycle arrest by CP-358,774, an inhibitor of epidermal growth factor receptor tyrosine kinase. Cancer Res 1997;57:4838–48.
12. Pollack VA, Savage DM, Baker DA, et al. Inhibition of epidermal growth factor receptor-associated tyrosine phosphorylation in human carcinomas with CP-358,774: dynamics of receptor inhibition *in situ* and antitumor effects in athymic mice. J Pharmacol Exp Ther 1999;291: 739–48.
13. Albanell J, Rojo F, Baselga J. Pharmacodynamic studies with the epidermal growth factor receptor tyrosine kinase inhibitor ZD1839. Semin Oncol 2001;28: 56–66.
14. Shepherd FA, Rodrigues Pereira J, Ciuleanu T, et al. Erlotinib in previously treated non-small-cell lung cancer. N Engl J Med 2005;14:123–32.
15. Giaccone G, Herbst RS, Manegold C, et al. Gefitinib in combination with gemcitabine and cisplatin in advanced non-small-cell lung cancer: a phase III trial-INTACT 1. J Clin Oncol 2004;22:777–84.
16. Herbst RS, Giaccone G, Schiller JH, et al. Gefitinib in combination with paclitaxel and carboplatin in advanced non-small-cell lung cancer: a phase III trial-INTACT 2. J Clin Oncol 2004;22:785–94.
17. Lynch TJ, Bell DW, Sordella R, et al. Activating mutations in the epidermal growth factor receptor underlying responsiveness of non-small-cell lung cancer to gefitinib. N Engl J Med 2004;350:2129–39. Epub 2004 Apr 29.
18. Paez JG, Janne PA, Lee JC, et al. EGFR mutations in lung cancer: correlation with clinical response to gefitinib therapy. Science 2004;304:1497–500. Epub 2004 Apr 29.
19. Jones HE, Goddard L, Gee JM, et al. Insulin-like growth factor-I receptor signalling and acquired resistance to gefitinib (ZD1839; Iressa) in human breast and prostate cancer cells. Endocr Relat Cancer 2004;11: 793–814.
20. Liu B, Fang M, Lu Y, Mendelsohn J, Fan Z. Fibroblast growth factor and insulin-like growth factor differentially modulate the apoptosis and G1 arrest induced by anti-epidermal growth factor receptor monoclonal antibody. Oncogene 2001;20:1913–22.
21. Altieri DC. Survivin and apoptosis control. Adv Cancer Res 2003;88:31–52.
22. Lee CT, Park KH, Adachi Y, et al. Recombinant adenoviruses expressing dominant negative insulin-like growth factor-I receptor demonstrate antitumor effects on lung cancer. Cancer Gene Ther 2003;10:57–63.
23. Lee HY, Moon H, Chun KH, et al. Effects of insulin-like growth factor binding protein-3 and farnesyltransferase inhibitor SCH66336 on Akt expression and apoptosis in non-small-cell lung cancer cells. J Natl Cancer Inst 2004;96:1536–48.
24. Goldstein D, Bushmeyer SM, Witt PL, Jordan VC, Borden EC. Effects of type I and II interferons on cultured human breast cells: interaction with estrogen receptors and with tamoxifen. Cancer Res 1989;49: 2698–702.
25. Chun KH, Kosmeder JW II, Sun S, et al. Effects of deguelin on the phosphatidylinositol 3-kinase/Akt pathway and apoptosis in premalignant human bronchial epithelial cells. J Natl Cancer Inst 2003;95:291–302.
26. Parrizas M, Gazit A, Levitzki A, Wertheimer E, LeRoith D. Specific inhibition of insulin-like growth factor-1 and insulin receptor tyrosine kinase activity and biological function by tyrphostins. Endocrinology 1997; 138:1427–33.
27. Peterson RT, Desai BN, Hardwick JS, Schreiber SL. Protein phosphatase 2A interacts with the 70-kDa S6 kinase and is activated by inhibition of FKBP12-rapamycinassociated protein. Proc Natl Acad Sci U S A 1999;96:4438–42.
28. Chakravarti A, Loeffler JS, Dyson NJ. Insulin-like growth factor receptor I mediates resistance to anti-epidermal growth factor receptor therapy in primary human glioblastoma cells through continued activation of phosphoinositide 3-kinase signaling. Cancer Res 2002; 62:200–7.
29. Balana ME, Labriola L, Salatino M, et al. Activation of ErbB-2 via a hierarchical interaction between ErbB-2 and type I insulin-like growth factor receptor in mammary tumor cells. Oncogene 2001;20:34–47.
30. Gilmore AP, Valentijn AJ, Wang P, et al. Activation of BAD by therapeutic inhibition of epidermal growth factor receptor and transactivation by insulin-like growth factor receptor. J Biol Chem 2002;277:27643–50. Epub 2002 May 13.
31. Ahmad T, Farnie G, Bundred NJ, Anderson NG. The mitogenic action of insulin-like growth factor I in normal human mammary epithelial cells requires the epidermal growth factor receptor tyrosine kinase. J Biol Chem 2004;279:1713–9. Epub 2003 Oct.
32. Kuribayashi A, Kataoka K, Kurabayashi T, Miura M. Evidence that basal activity, but not transactivation, of the epidermal growth factor receptor tyrosine kinase is required for insulin-like growth factor I-induced

activation of extracellular signal-regulated kinase in oral carcinoma cells. Endocrinology 2004;145:4976–84. Epub 2004 Jul 22.
33. Holcik M, Gibson H, Korneluk RG. XIAP: apoptotic brake and promising therapeutic target. Apoptosis 2001; 6:253–61.
34. Gingras AC, Gygi SP, Raught B, et al. Regulation of 4E-BP1 phosphorylation: a novel two-step mechanism. Genes Dev 1999;13:1422–37.
35. Herbst RS. Erlotinib (Tarceva): an update on the clinical trial program. Semin Oncol 2003;30:34–46.
36. Amann J, Kalyankrishna S, Massion PP, et al. Aberrant epidermal growth factor receptor signaling and enhanced sensitivity to EGFR inhibitors in lung cancer. Cancer Res 2005;65:226–35.
37. Tracy S, Mukohara T, Hansen M, Meyerson M, Johnson BE, Janne PA. Gefitinib induces apoptosis in the EGFRL858R non-small-cell lung cancer cell line H3255. Cancer Res 2004;64:7241–4.
38. Roskoski R, Jr. The ErbB/HER receptor protein-tyrosine kinases and cancer. Biochem Biophys Res Commun 2004;319:1–11.
39. Garrett TP, McKern NM, Lou M, et al. Crystal structure of the first three domains of the type-1 insulin-like growth factor receptor. Nature 1998;394: 395–9.
40. Jimeno A, Rubio-Viqueira B, Amador ML, et al. Epidermal growth factor receptor dynamics influences response to epidermal growth factor receptor targeted agents. Cancer Res 2005;65:3003–10.
41. Tan AR, Yang X, Hewitt SM, et al. Evaluation of biologic end points and pharmacokinetics in patients with metastatic breast cancer after treatment with erlotinib, an epidermal growth factor receptor tyrosine kinase inhibitor. J Clin Oncol 2004;22:3080–90.
42. Gregorc V, Ceresoli GL, Floriani I, et al. Effects of gefitinib on serum epidermal growth factor receptor and HER2 in patients with advanced non-small cell lung cancer. Clin Cancer Res 2004;10:6006–12.
43. Rao RD, Mladek AC, Lamont JD, et al. Disruption of parallel and converging signaling pathways contributes to the synergistic antitumor effects of simultaneous mTOR and EGFR inhibition in GBM cells. Neoplasia 2005;7:921–9.
44. Gschwind A, Zwick E, Prenzel N, Leserer M, Ullrich A. Cell communication networks: epidermal growth factor receptor transactivation as the paradigm for interreceptor signal transmission. Oncogene 2001;20: 1594–600.
45. Roudabush FL, Pierce KL, Maudsley S, Khan KD, Luttrell LM. Transactivation of the EGF receptor mediates IGF-1-stimulated shc phosphorylation and ERK1/2 activation in COS-7 cells. J Biol Chem 2000; 275:22583–9.
46. Pierce KL, Luttrell LM, Lefkowitz RJ. New mechanisms in heptahelical receptor signaling to mitogen activated protein kinase cascades. Oncogene 2001;20: 1532–9.
47. Marinissen MJ, Gutkind JS. G-protein-coupled receptors and signaling networks: emerging paradigms. Trends Pharmacol Sci 2001;22:368–76.
48. Pollak M. Insulin-like growth factor physiology and cancer risk. Eur J Cancer 2000;36:1224–8.
49. Merrill MJ, Edwards NA. Insulin-like growth factor-I receptors in human glial tumors. J Clin Endocrinol Metab 1990;71:199–209.